

A novel specific and ultrasensitive method detecting extracellular vesicles secreted from lung cancer by padlock probe-based exponential rolling circle amplification



Lei He^{a,b}, Xiaocheng Yu^a, Rongrong Huang^b, Lian Jin^c, Yuan Liu^a, Yan Deng^c, Song Li^c, Hui Chen^c, Zhu Chen^c, Zhiyang Li^{b,*}, Pengfeng Xiao^{a,*}, Nongyue He^{a,c,**}

^a State Key Laboratory of Bioelectronics, School of Biological Science and Medical Engineering, National Demonstration Center for Experimental Biomedical Engineering Education (Southeast University), Southeast University, Nanjing 210096, PR China

^b Department of Clinical Laboratory, the Affiliated Drum Tower Hospital of Nanjing University Medical School, Nanjing 210008, PR China

^c Hunan Key Laboratory of Biomedical Nanomaterials and Devices; Hunan University of Technology, Zhuzhou 412007, PR China

ARTICLE INFO

Article history:

Received 22 June 2021

Received in revised form 21 September 2021

Accepted 28 October 2021

Available online 10 November 2021

Keywords:

Lung cancer

Extracellular vesicles

Aptamer

Fluorescence

Rolling circle amplification

ABSTRACT

Lung cancer is one of the most common cancers in the world. Early diagnosis of lung cancer usually shows promising rate of survival. However, the detection of lung cancer faces great challenges. Transthoracic needle biopsy combined with image-guidance will make patients suffer from some damages. Liquid biopsy can be used as an auxiliary method for early diagnosis and prognosis of cancers owing to its minimally invasive performance. Proteins on the surface of Extracellular vesicles (EVs) derived from lung cancer are used as biomarkers for cancers. Here, a highly specific and sensitive fluorescence scheme based on padlock probe-based exponential rolling circle amplification (P-ERCA) assay for detecting extracellular vesicles was reported. The aptamer against extracellular vesicles derived from lung cancer cells was linked to a primer sequence (aptamer-primer complex) that was complementary to padlock probe. The padlock probe was composed of a nicking site for nicking endonuclease. At the presence of target extracellular vesicles, aptamer-primer complex could trigger linear rolling circle amplification (LRCA) under isothermal conditions. After multiple nicking reactions, many copies of single-stranded DNAs (trigger DNA) were produced and leading to another circle amplification. The exponential fluorescence signal of P-ERCA product dyed with SYBR Green II was detected. The method exhibits high specific and sensitivity to lung cancer extracellular vesicles with low detection limit of 4.222×10^4 particles/mL, and the linear range is 5×10^4 particles/mL– 1.2×10^6 particles/mL. Furthermore, this method could successfully distinguish the signal of extracellular vesicles in real human serum sample between 17 lung cancer patients and 17 healthy persons ($P < 0.001$).

© 2021 Elsevier Ltd. All rights reserved.

Introduction

Lung cancer is one of the malignancies associated with death in the world [1]. The 5-year survival rate of lung cancer is only 11–18% currently [2]. The lack of efficient biomarkers and the lack of accurate detecting method are important reasons of the low survival rate (<25%) [3,4]. Transthoracic needle biopsy combined with image-

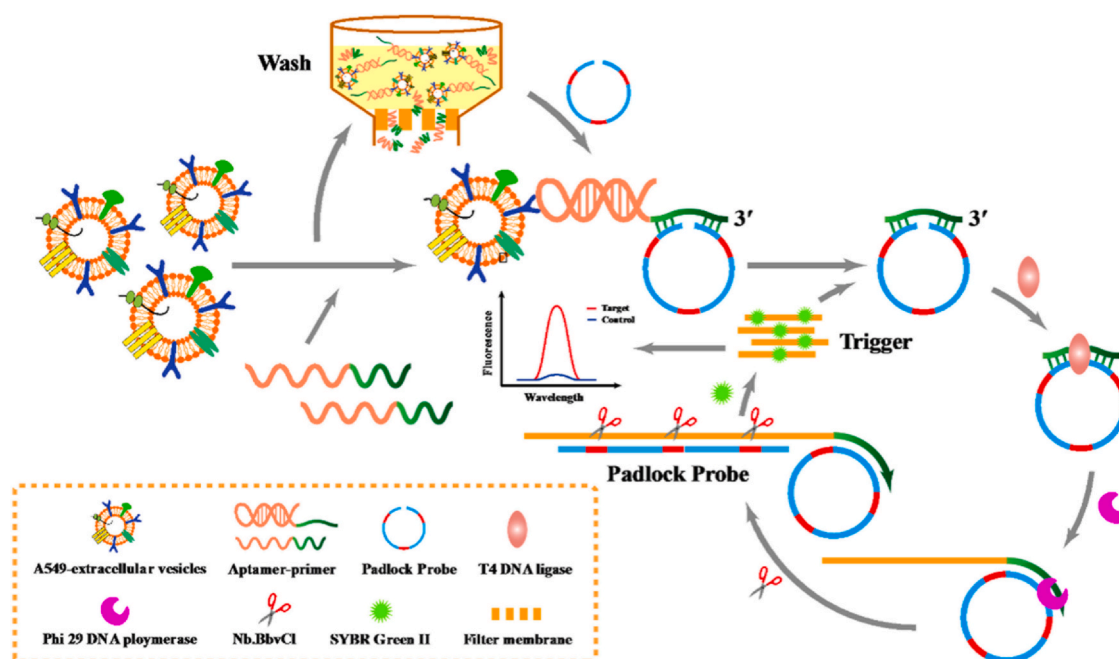
guidance is widely used for patients with a solitary lung nodule, for diagnosis of lung malignancy or for molecular testing of the tumor [5]. However, imaging examination with low sensitivity is difficult to detect small tumor, and the patients will suffer from some damages when treated with the transthoracic needle biopsy and, therefore, it is not suitable for repeated examination and diagnosis [5].

Liquid biopsy can be used as an auxiliary method for early diagnosis and prognosis of cancers owing to its minimally invasive performance. Extracellular vesicles (EVs) as an emerging liquid biopsy for the diagnosis and treatment are attracting great attention [6–8]. The proteins are the main executors of biological functions and are especially rich in EVs which is of great significance to analyze the specific role of EVs in tumor and clinical diagnosis [9]. Currently, a lot of novel detecting techniques based on aptamers have been established to research the proteins on the surface of EVs.

* Corresponding authors.

** Corresponding author at: State Key Laboratory of Bioelectronics, School of Biological Science and Medical Engineering, National Demonstration Center for Experimental Biomedical Engineering Education (Southeast University), Southeast University, Nanjing 210096, PR China.

E-mail addresses: lizhiyangcn@qq.com (Z. Li), xiaopf@seu.edu.cn (P. Xiao), nyhe1958@163.com (N. He).



Scheme 1. The reaction involved five principal steps: (1) The EVs were incubated with aptamer-primer; (2) The mixture was washed with PBS and the A549-EVs-aptamer-primer was obtained; (3) The padlock probe was ligated specifically and circularized with the aptamer-primer as template in the presence of T4 DNA ligase; (4) A long repetitive sequence of the padlock probe was synthesized by Phi29 DNA polymerase; (5) Multiple padlock probe could be hybridized to the DNA product. The nicking sites of sequences were recognized and cleaved by Nicking endonuclease. Multiple triggers were produced and a new reaction cycle was initiated. Through multiple reaction cycles and the sequence dyed by SYBR Green II, an exponential fluorescence signal for a small amount of EVs was detected.

These methods are designed based on different detecting principles, such as colorimetry [10], fluorescence method [11,12], surface enhanced Raman scattering [13], surface plasmon resonance [14,15] and electrochemistry method [16–23]. Although EVs can be detected accurately and quantitatively by the newly developed methods, these methods still have some drawbacks. Although the sensitivity of some methods are very high, the process of cleaning procedure complicated, and there are certain difficulties in clinical application [24,25].

In order to solve these problems, we develop a fluorescent method by taking advantages of aptamer and padlock probe-based exponential rolling circle amplification (P-ERCA) for detection of EVs derived from Lung cancer. The principle of this method was shown in Scheme 1. A specific aptamer had been designed for recognizing target EVs and initiating the ligation reaction of P-ERCA. The used aptamer was only bound to A549-EVs but not to EVs secreted from other tumor. A small number of A549-EVs could be detected by this method for signal amplification. Herein, this method has excellent specificity, high sensitivity and reproducibility. A series of experiments show this exponential signal amplification method provides a convenient tool for further applications in early lung cancer diagnosis.

Experimental section

Materials and apparatus

DNA sequences were purchased from Sangon Biological Engineering Technology & Services Co., Ltd (Shanghai, China). T4 DNA ligase, Phi29 DNA polymerase, and Nb.BbvCI were purchased from New England Biolabs (Ipswich, MA). SYBR Green II (10000 ×), BSA, diethylprocarbonated (DEPC) treated water and TE buffer were purchased from Sangon Biological Engineering Technology & Services Co., Ltd (Shanghai, China). Deoxynucleotides (dNTPs), and Phosphate-buffered saline (PBS) were obtained from TaKaRa Biotechnology Co., Ltd. (Dalian, China). Dulbecco's modified Eagle's

medium (DMEM, high glucose), Roswell Park Memorial Institute 1640 (RPMI 1640, high glucose), and fetal bovine serum (FBS) were purchased from Gibco (Invitrogen). Exosome-depleted FBS Media Supplement was purchased from System Biosciences, SBI (CA, USA). Penicillin-streptomycin was purchased from Sigma-Aldrich. All cell lines were purchased from the Nanjing Kebai Biotechnology Co., Ltd (Nanjing, China). The used DNA sequences were listed in Table 1, aptamer (Ap6) was acquired by EVs-SELEX (Aptamers specially recognizing the proteins of EVs were selected based on the Systematic Evolution of Ligands by Exponential Enrichment, EVs-SELEX) [26]. Gel electrophoresis was detected using automatic gel imaging analyzer (JS-680D, Shanghai PeiQing, China) and ChemiScope3300Mini chemiluminescence imaging system (Science Instruments, China). The fluorescent spectra were measured using Shimadzu RF-6000 spectrofluorometer (Shimadzu (China) Co., Ltd.). Nanoparticle Tracking Analysis (NTA, NanoSight NS300) was purchased from Malvern Instruments Ltd. Transmission electron microscope (TEM, JEM-2100) was purchased from Japan. The fluorescence was determined with DxFLEX flow cytometry (Beckman Coulter, Inc.).

Aptamer-primer probe includes the aptamer Ap6 sequence (black) against A549-EVs and the universal primer sequence (blue and green). Padlock probe includes the hybridization sequence that is complementary to the primer (blue and green) and the recognition sequences of Nb.BbvCI (red).

Cell culture and preparation of EVs

A549 cells (human non-small lung cancer cell line) were cultured in 1640 medium, Beas-2b cells (human lung epithelial cells) were cultured in DMEM medium. BGC-823 (human gastric cancer cell line), Caco-2 (human colon adenocarcinoma cell), SK-BR-3 (human breast cancer cell) and HepG2 (human liver hepatoma cell) were cultured in corresponding medium. All media were supplemented with 10% fetal bovine serum (FBS) and 1% penicillin-streptomycin. All cell lines were incubated in a humidified incubator at 37 °C with a 5% CO₂ atmosphere respectively. After all cells grew to 70–80%

Table 1
Sequences of oligonucleotides.

Name	Sequence
Aptamer-primer[26]	5'-GTTGGTGAGGTAACGGCTCAACAGGGGTTTCGGTAGTCGTGTGGTTTCGGTTG GGTGTAGTTAGTGGCAAGCGTTATCCGTGAGGTAGTAGGTTGTATAGTT-3'
Padlock probe	5'-phosphate-CTACTACCTCACCTCAGCAACTATACAACCTACTACCTCACCTC AGCAACTATACAACCTACTACCTCACCTCAGCAACTATACAAC-3'

confluence, cells were washed twice with PBS and incubated for 48 h in the medium containing 10% exosome-depleted FBS. Then, the culture medium was collected and centrifuged at 4 °C (2000 g for 15 min and 10,000 g for 30 min) to remove intact cells or cellular debris. The acquired culture solution was filtered through a 600 nm of track-etched polycarbonate filter membrane and 20 nm of anopore filter membrane (Size-Selective Method, SSM) [27]. The obtained EVs were resuspended in PBS.

Purified EVs were adsorbed on carbon-coated copper grids and confirmed by TEM at 80 kVs. EVs were dropped on carbon-coated copper grids and used to capture the anti-CD63 gold which bound on EVs specially. The compound was detected by TEM. The size distribution and concentration of EVs were quantified by NTA. The surface protein of EVs were analyzed by western blot.

EVs Modified with aptamer-primer probe

Purified EVs were incubated with aptamer-primer probes in 1 mL of binding buffer (BB) for 1 h at 4 °C. After washing thrice with PBS to remove the unbound aptamer-primer probe by SSM, the complex 150 μ L of EVs-aptamer-primer was obtained.

Ligation reactions

The acquired 8.4 μL of above liquid and 0.3 μL of 10 μM padlock probe were denatured at 65 $^{\circ}\text{C}$ for 3 min and cooled slowly to room temperature over (10 min). Then, 1 μL of 10 \times T4 DNA ligase buffer and 0.3 μL of T4 DNA ligase (350 U/ μL) were added, and the suspension liquid was incubated at 37 $^{\circ}\text{C}$ for 2 h in a PCR tube.

RCA detection based on fluorescent

10 μ L of ligation reaction products, 2 μ L of 10 \times Phi29 DNA polymerase buffer, 1 μ L of dNTP, 0.4 μ L of BSA, 0.8 μ L of Phi29 DNA polymerase (10 U/ μ L), 0.5 μ L of Nb.BbvCl (10 U/ μ L) and 5.3 μ L of H₂O were mixed and incubated for 6 h at 30 $^{\circ}$ C for amplifying reaction. Enzymes were inactivated for 10 min at 65 $^{\circ}$ C. 6 μ L of the amplified products and 4 μ L of 20 \times SYBR Green II was added in 590 μ L of PBS. The fluorescence intensity was recorded by Hitachi F-4500 spectrofluorometer. The excitation wavelength was 480 nm, and the fluorescence spectra were recorded from 520 nm to 650 nm.

Gel electrophoresis analysis of P-ERCA products

Agarose gel electrophoresis (AGE) was used to analyze the P-ERCA product. The gel was carried in 1 × electrophoresis Tris-borate-EDTA (TBE) at room temperature under 100 V for 50 min. The imaging of the gel was measured by automatic gel imaging analyzer.

Clinical sample analysis

The blood of 17 samples from lung cancer patients with staged I and the blood of 17 samples from healthy persons (collected in EDTA-anticoagulated tubes) were provided by Affiliated Drum Tower Hospital of Nanjing University Medical School. All patients and volunteers gave informed consent. The study was approved by the ethic committee of the Affiliated Drum Tower Hospital of Nanjing

University Medical School. After standing 1 h, the supernatant liquid was transferred into a centrifuge tube. The blood samples were centrifuged at 1000 g for 10 min, and then 1500 g for 15 min. Then, the dealt original serum was used as samples for detecting directly.

Flow cytometry analysis

The flow cytometry analysis was used to investigate the binding ability of the selected aptamers with EVs derived from A549 and Beas-2b. The FITC-labeled ssDNA pool or aptamers were incubated with A549-EVs or Beas-2b-EVs at 4 °C for 1 h in 1 mL of binding buffer respectively. Then, the EVs were washed thrice by washing buffer and resuspended in 300 μ L of PBS for cytometric test by using flow cytometer.

Results and discussion

Principle of EVs assay based on P-ERCA

The principle of EVs detection based on the padlock probe exponential rolling circle amplification (P-ERCA) is illustrated in [Scheme 1](#).

According to their different functions, the aptamer-primer complexes are designed into two domains termed as I and II. Region I (GTTGGTGAGGTAACGGCTCAACAGGGGTTTCGGTAGTCGTGTGGTTTCGGTTGGGTGTAGTTAGGTGGCAAGCGTTATCCG) is the sequence of the aptamer recognized A549-EVs (black sequence of aptamer-primer in [Table 1](#)). Region II (TGAGGTAGTAGGTTGTATAGTT (blue and green sequences of aptamer-primer in [Table 1](#)) is a universal primer sequence, which could serve not only as the primer for the RCA reaction but also as the template for padlock probe ligation. The padlock probe has two functional units named as III and IV. Region III (AACTATACAACCTACTACCTCA) (blue and green sequences of padlock probe in [Table 1](#)) contains the hybridization sequence that is complementary to the primer. Region IV (CCTCAGC) (red sequences of padlock probe in [Table 1](#)) is a binding site of nicking endonuclease (Nb.BbvCI) which can be cleaved under the formation of the double-stranded DNA. Both the 3'- and 5'-terminus of a padlock probe could hybridize to the 3'-terminus of the aptamer-primer. At the presence of target EVs, the aptamer-primer is combined on the EVs specifically. After washed with PBS by means of SSM, only the target EVs had aptamer-primer on their surface. The primer contained in aptamer-primer as a template hybridized with padlock probe to form a duplex structure and form a circular template in the presence of T4 DNA ligase. After adding the Phi29 DNA polymerase and dNTPs, primer can trigger the RCA reaction and a long concatenated sequence copy of the padlock probe will be synthesized through linear rolling circle amplification. Followed, a number of padlock probes can hybridize to suitable sites of the LRCA DNA product, and nicking endonuclease recognizes the sites and cleaves the double-stranded DNA at specific sites to release multiple short DNA products as new triggers to initiate multiple reaction cycles. Meanwhile, the padlock probe is also released and recycled for next reaction. The reaction will be terminated after the depleting of reaction components, such as dNTP substrates. Therefore, LRCA will convert to an exponential amplification (ERCA) with the cycles of LRCA and cleavage repeating continuously. Finally, a large number

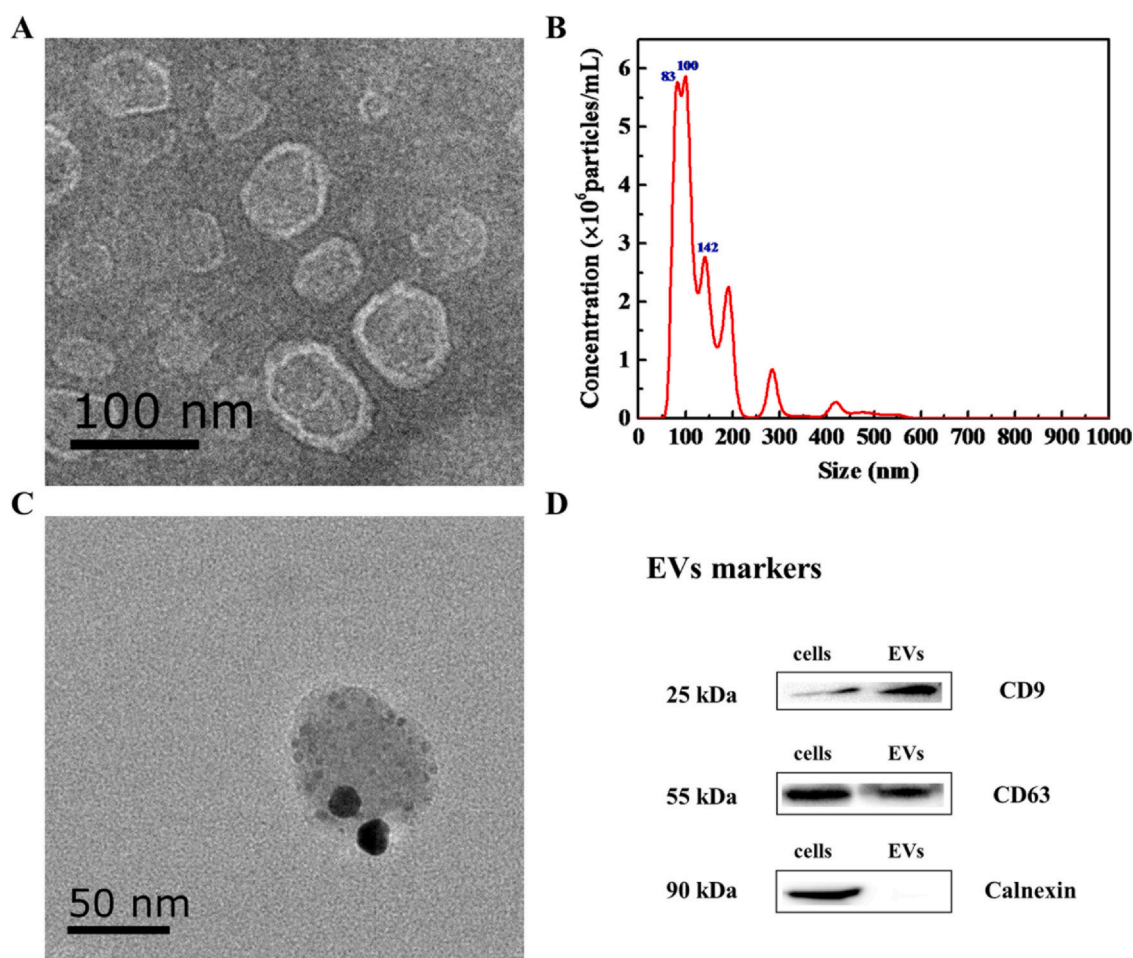


Fig. 1. The characterization of EVs derived from A549 cells. (A) TEM image of EVs; (B) Nanoparticle tracking analysis (NTA) of EVs; (C) Immunoelectron microscopy showed that the anti-CD63 gold was stained on EVs; (D) Western blotting analysis of the expression of CD9, CD63 and Calnexin proteins on the surface of A549 cells and A549-EVs.

of long single-stranded DNA will be dyed with SYBR Green II and the amplified fluorescent signal will be detected by fluorescence spectrophotometer.

Characterisation of EVs

In order to ensure the EVs were isolated successfully, the EVs were investigated by TEM, NTA, western blot analysis and immunogold labeling. The EVs displayed a cup-shaped morphology and the diameter was between 30 and 200 nm observed by TEM (Fig. 1A). NTA (Fig. 1B) confirmed that the sizes of the most EVs were around 100 nm. The result was in agreement with the microscopy images. The anti-CD63 gold could be bound on EVs and the appearance indicated that CD63 existed on the surface of EVs (Fig. 1C). Western blot analysis demonstrated that CD9 and CD63 were expressed in EVs and cells. In addition, calnexin was only detected in cells and was not detected in EVs (Fig. 1D) [28–31]. These results proved that the extracted vesicles were EVs.

Specificity of aptamers (Ap6)

The binding of FAM-labeled Ap6 to A549-EVs and Beas-2b-EVs was tested by flow cytometry. As shown in Fig. 2, Ap6 only bound to A549- EVs and did not bind to Beas-2b-EVs. Similar to the proteomics analysis [32], aptamers represented by the EVs-SELEX

technique could also be used as a tool to distinguish tumor EVs from normal cell EVs. This experiment demonstrated that the Ap6 could recognize the target EVs derived from lung cancer. The high specificity made Ap6 has the potential for application in P-ERCA.

Feasibility of strategy for EVs detection

The principle of P-ERCA-Based Method was verified by the detection of fluorescent spectra and 0.8% agarose gel electrophoresis. Fig. 3A showed that the fluorescence intensity gradually increases in the presence of aptamer-primer (curve a), demonstrating that the padlock probe formed to ring with the help of T4 DNA ligase, P-ERCA was triggered and a large number of DNA products were generated. The fluorescence intensity was weak without aptamer-primer (curve b), indicating that no reaction occurred. The analysis of gel electrophoresis was performed for further validation of the principle. As shown in Lane 1 (Fig. 3B), the band at the nearby position of charging aperture was very bright. This demonstrated that abundant of high-molecular-weight DNA was produced, and the band was wide attributing to the multiple components of the cleavage. This might be that the linear rolling ring product had nicking sites every 22 bases [33]. No band was observed at the absence of aptamer-primer (lane 2 in Fig. 3B) indicating that no DNA products existed. This was probably because that no circular template was formed and the P-ERCA could not be carried out. The two results proved that the

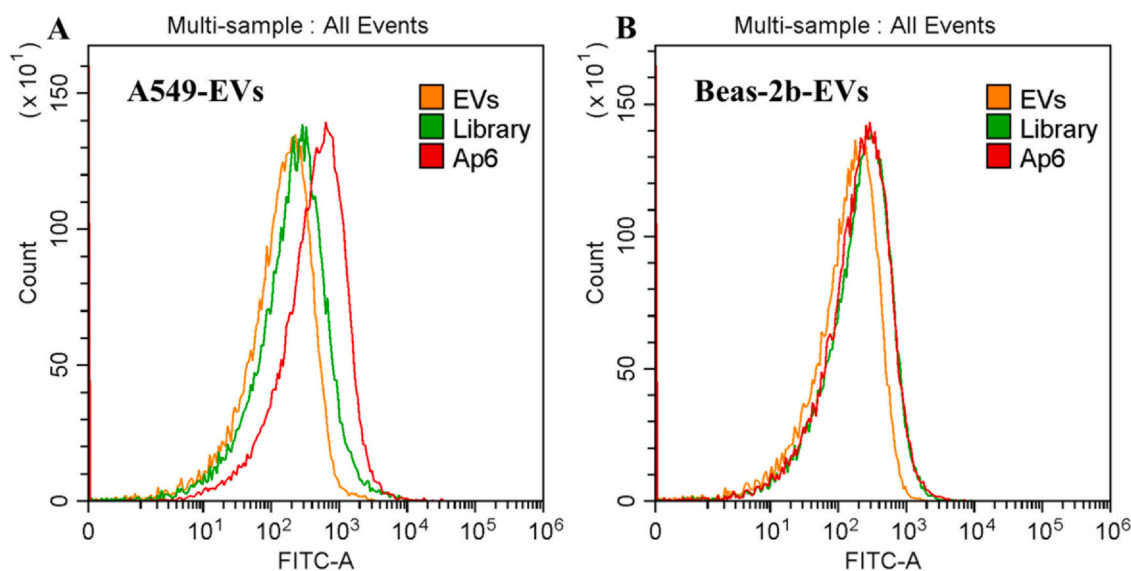


Fig. 2. Flow cytometric assay of the binding capacity of the aptamer. (A) Binding assay of Ap6 to A549-EVs; (B) Binding assay of Ap6 to Beas-2b-EVs. Only corresponding EVs were used as blank control, FAM-labeled unselected DNA library was used as the negative control.

principle of designed method based on P-ERCA was feasible and could be used for the subsequent experiment.

Optimization of reaction conditions based on P-ERCA

To obtain the optimum analytical performance for detecting of EVs sensitively, several parameters were investigated, including the ratio of aptamer-primer to padlock probe, the concentrations of dNTP substrates, Phi29 DNA polymerase, and nicking enzyme Nb.BbvCI; the reaction time of P-ERCA. The concentrations of dNTP, Phi29 DNA polymerase and nicking enzyme Nb.BbvCI were found to be the key factors to affect the trigger DNA amplification.

In this experiment, different ratios (1:1, 1:2, 1:3, 2:1, 3:1) of aptamer-primer to padlock probe were designed to ensure the best reacting condition. The value of fluorescence was the highest when the ratio was 1:1 at 528 nm (Fig. 4A). Fig. 4B showed the values of fluorescence at different ratios (each ratio was detected for three times).

In order to optimize the concentration of dNTP, 100 μ M, 250 μ M, 500 μ M, 600 μ M, 750 μ M and 1000 μ M dNTP were designed. Fig. 5A

showed the variance of the F-F0 value with the concentration of dNTP. F and F0 were the fluorescence intensities in the presence and in the absence of EVs, respectively. With the concentration of dNTP increased, the F/F0 value increased gradually and decreased beyond 600 μ M dNTP. This phenomenon might be attributed to the spatial steric effect and limited space. Thus, 600 μ M dNTP was used in the subsequent research.

The relationship of fluorescence signals with the concentration of phi29 DNA polymerase was assessed. As shown in Fig. 5B, the F-F0 value (F and F0 were the fluorescence intensities in the presence and in the absence of EVs, respectively) increased with the increase in the concentration of phi29 DNA polymerase from 2 U to 8 U, decreasing from 8 U to 20 U. Therefore, 8 U phi29 DNA polymerase was selected in the following research.

In this method, a nicking enzyme Nb.BbvCI was used to cleave the DNA synthesized by linear RCA to trigger exponential amplification. So, the concentration of Nb.BbvCI should be optimized too. The data was shown in Fig. 5C. The F-F0 value increased with the increase in Nb.BbvCI from 2 U to 5 U, and the F-F0 value reached the

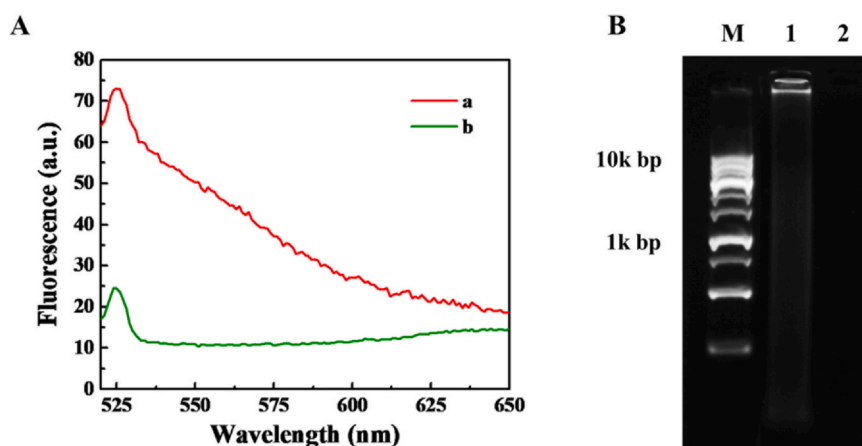


Fig. 3. The amplification products of P-ERCA were characterized by fluorescence intensity and 0.8% agarose gel electrophoresis. A: The fluorescence intensity in the presence (a) and absence (b) of aptamer-primer. B: M: DNA Marker (250–10,000 bp); 1: The result of P-ERCA in the presence of aptamer-primer; 2: The result of P-ERCA in the absence of aptamer-primer.

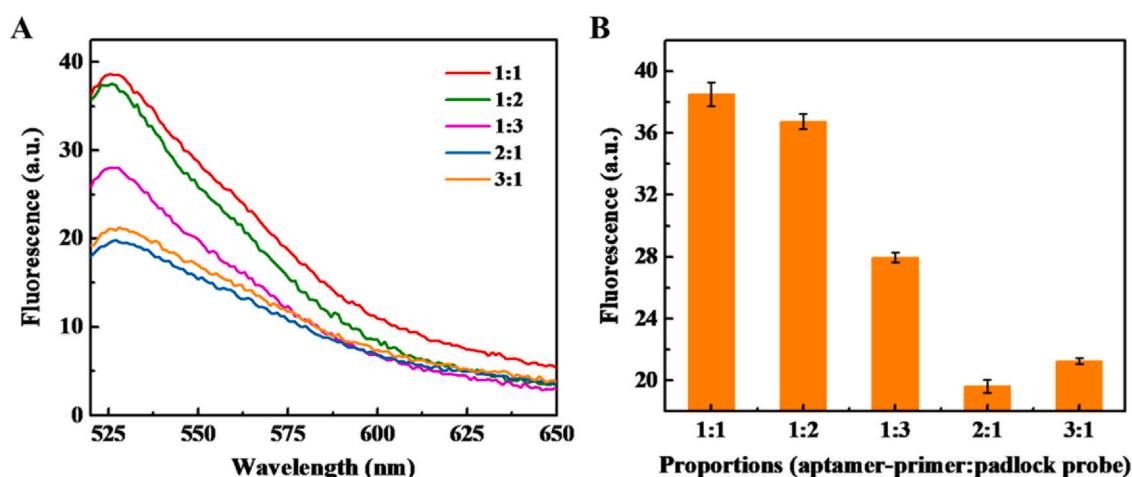


Fig. 4. The fluorescence values of amplified products under different proportions of aptamer-primer to padlock probe. (A) The result was analyzed by fluorescence spectrogram; (B) The result was analyzed by histogram of at peak value. The error bars were the standard deviation of three repetitive experiments.

maximum platform at 5 U (F and F0 were the fluorescence intensities in the presence and in the absence of EVs, respectively). Thus, 5 U Nb.BbvCI was used in the coming research.

To generate a long DNA sequence for signal amplification, the effect of the reaction time was further studied, which was shown in Fig. 5D. The F-F0 value (F and F0 were the fluorescence intensities in the presence and in the absence of EVs, respectively) increased steadily from 4 h to 6 h and then reached a plateau from 6 h to 10 h.

This might be explained by the exhaustion of substrate or production inhibition. Hence, 6 h was used for adequate reaction time in this experiment.

Specificity of the P-ERCA-based method for detection of EVs

The detection specificity was one of vital factors to evaluate the method for detecting EVs in practical application. Because of the method

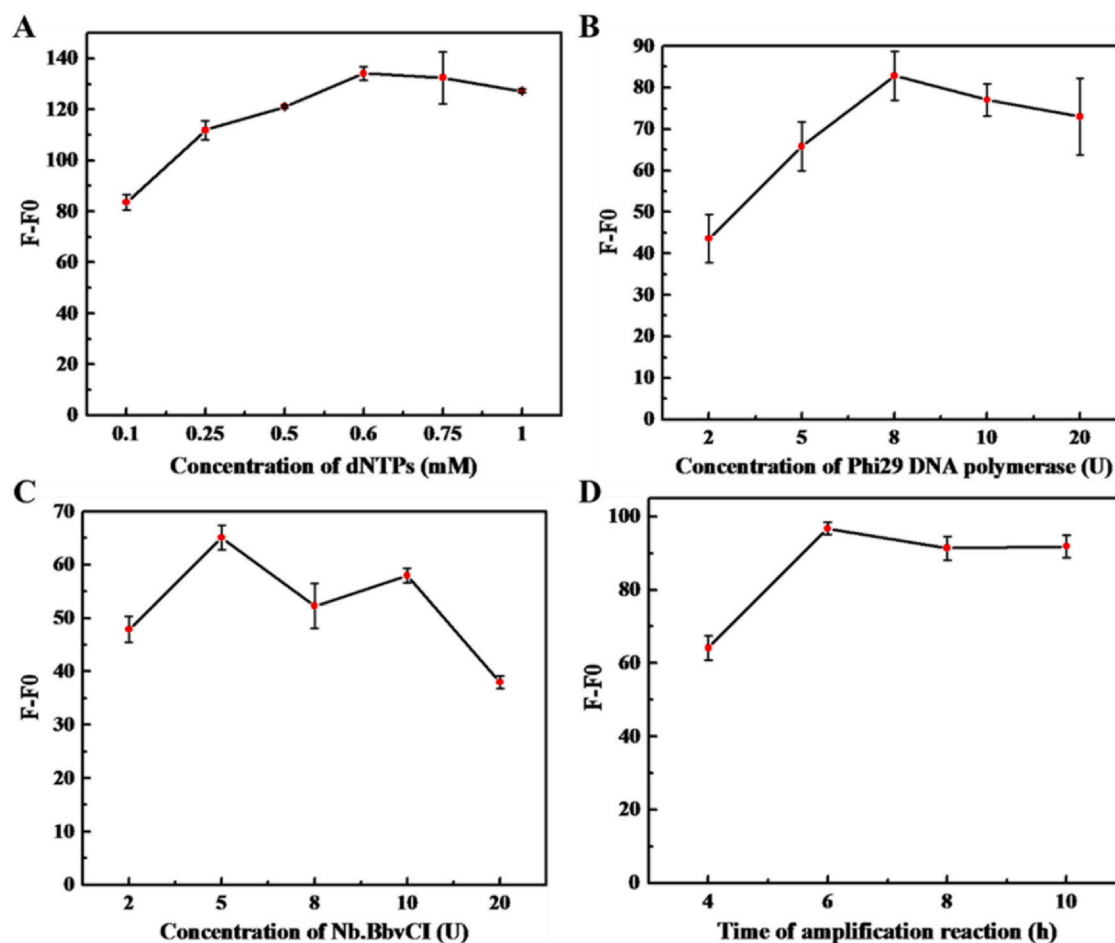


Fig. 5. The relationship between the fluorescence intensity and different conditions of P-ERCA: (A) concentration of dNTPs; (B) concentration of phi29 DNA polymerase; (C) concentration of Nb.BbvCI; (D) time of amplification reaction. The error bars were the standard deviation of three repetitive experiments.

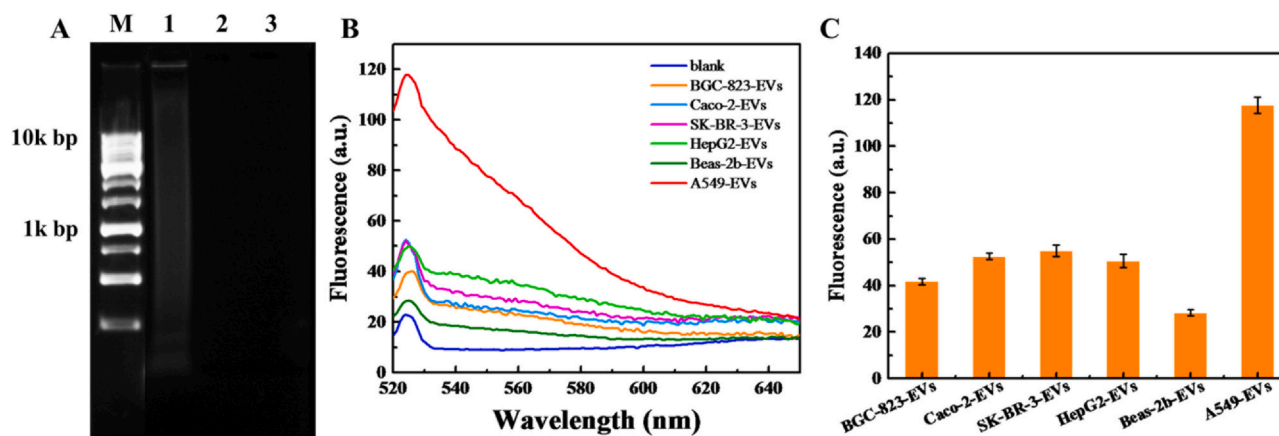


Fig. 6. Selectivity of method for detecting A549-EVs. (A) Agarose gel electrophoresis image of the products of P-ERCA. M: DNA Marker (250–10,000 bp); 1: The result of P-ERCA in the presence of A549-EVs; 2: The result of P-ERCA in the presence of Beas-2b-EVs; 3: blank; (B) the fluorescence intensity of different EVs derived from different cells respectively and blank; (C) The detecting result of different EVs was analyzed by histogram at peak value. The error bars were the standard deviation of three repetitive experiments.

was designed based on the aptamer against A549-EVs, the specificity of aptamer was the originally factor to affect the detection efficiency [34]. The aptamer of A549-EVs had been proved to specifically identify the target, but the aptamer used in this method had been changed by lengthening the sequence, which may lead to a variation in its recognition ability. In order to investigate the specificity of the approach for EVs, different EVs secreted from various cells such as BGC-823-EVs, Caco-2-EVs, SK-BR-3-EVs, HepG2-EVs and Beas-2b-EVs were selected and detected by using this new method under the same conditions. There was a bright amplification band in lane 1 of Fig. 6A, indicating the occurrence of P-ERCA process with A549-EVs. As the comparison, no product was observed in lane 2 of Fig. 6A, suggesting no amplification reaction occurred with Beas-2b-EVs. Fig. 6B and C displayed the comparison of fluorescence intensity in response to different kinds of target EVs. Conspicuously, the fluorescence value of A549-EVs was 4.15-fold higher than that of Beas-2b-EVs, 2.81-fold higher than that of BGC-823-EVs, 2.24-fold higher than that of Caco-2-EVs, 2.14-fold higher than that of SK-BR-3-EVs and 2.32-fold higher than that of HepG2-EVs. All fold satisfied the requirements of immunoassay (2.1 fold). These results demonstrated that this proposed method had high specificity and good selectivity to target EVs. It allowed for easy distinguish of targets EVs from other EVs. Such excellent selectivity was attributed to the high specificity and selectivity of the aptamer. Therefore, the method had a promising application in EVs analysis.

Sensitivity and reproducibility of EVs detection

Quantitative detection of EVs with high sensitivity is important for early diagnosis of lung cancer. Therefore, various concentrations of A549-EVs were measured to evaluate the sensitivity of the method under the optimal conditions. All experiments were repeated for three times. Fig. 7A showed the variance of fluorescence intensity with the concentration of target EVs. In the absence of A549-EVs, no observable fluorescence intensity was detected (blank control) because of no P-ERCA amplified and no ssDNA-SYBR Green II formed. The fluorescence intensity increased gradually with the increase in the concentration of A549-EVs from 0 particles/mL to 1×10^9 particles/mL, indicating that the concentration of A549-EVs could be easily reflected by the fluorescence intensity. This also illustrated that the continuous ssDNA and ssDNA-SYBR Green II were formed through P-ERCA. The peak at

528 nm was used as the criterion to judge the linear relation between fluorescence intensity and concentration of A549-EVs. Fig. 7B exhibited that fluorescence intensity at the peak increased gradually with the increase in the concentration of A549-EVs from 1×10^3 particles/mL to 1×10^9 particles/mL. Fig. 7C exhibited that fluorescence intensity had excellent linear correlation with the concentration of EVs over the range from 5×10^4 particles/mL to 1.2×10^6 particles/mL. The linear regression equation was $\Delta F = 36.542 + 8.038 \times 10^{-5}A$ with a correlation coefficient $R^2 = 0.99392$ ($\Delta F = F - F_0$, where F and F_0 were the fluorescence intensities with and without EVs, respectively, and C was the concentration of EVs). According to the ten times standard deviation principle, the limit of detection (LOD) was 4.222×10^4 particles/mL which has a detectable fluorescence change compared with the blank control. Apparently, the proposed method had desirable linear range and high sensitivity. The excellent sensitivity was mainly ascribed to the following aspects: the high amplification efficiency of the P-ERCA reaction and the amplified signal triggered by the repeated cleavage of the Nb.BbvCI nicking enzyme. Therefore, the low detection limit of the method allowed the sensitive detection of EVs at low concentrations.

The reproducibility of the method had been evaluated by detecting 1×10^8 particles/mL of EVs 5 reduplicate. The relative standard deviation (RSD) was 3.46%, displaying good reproducibility (Fig. 7D). Reproducibility is also a very important factor for clinical laboratory. There are two main advantages in this method, firstly the aptamers are very stable and have a long shelf life (several years). They can resist high temperature (even 95°C) and stand repeated cycles of denaturation and renaturation [35,36]. Secondly, fewer cleaning steps by using SSM in this methods ensure less EVs loss, thus ensuring the consistency of the experiment.

EVs are difficult to isolate compared with microRNA and telomeres. The SSM method can guarantee the integrity of vesicles to the maximum extent compared with hypervelocity centrifugation method. At the same time, A549-EVs-aptamer-primer can be separated easily from the free aptamer-primers that can reduce the background value. Although some rolling circle amplification strategies reported in detecting miRNAs and telomeres [37–39], the P-ERCA with aptamer and SSM technology was the first time to translated the information of EVs surface protein to fluorescence signal value. It made the operation of tumor EVs detecting very simple and more suitable for clinical diagnosis.

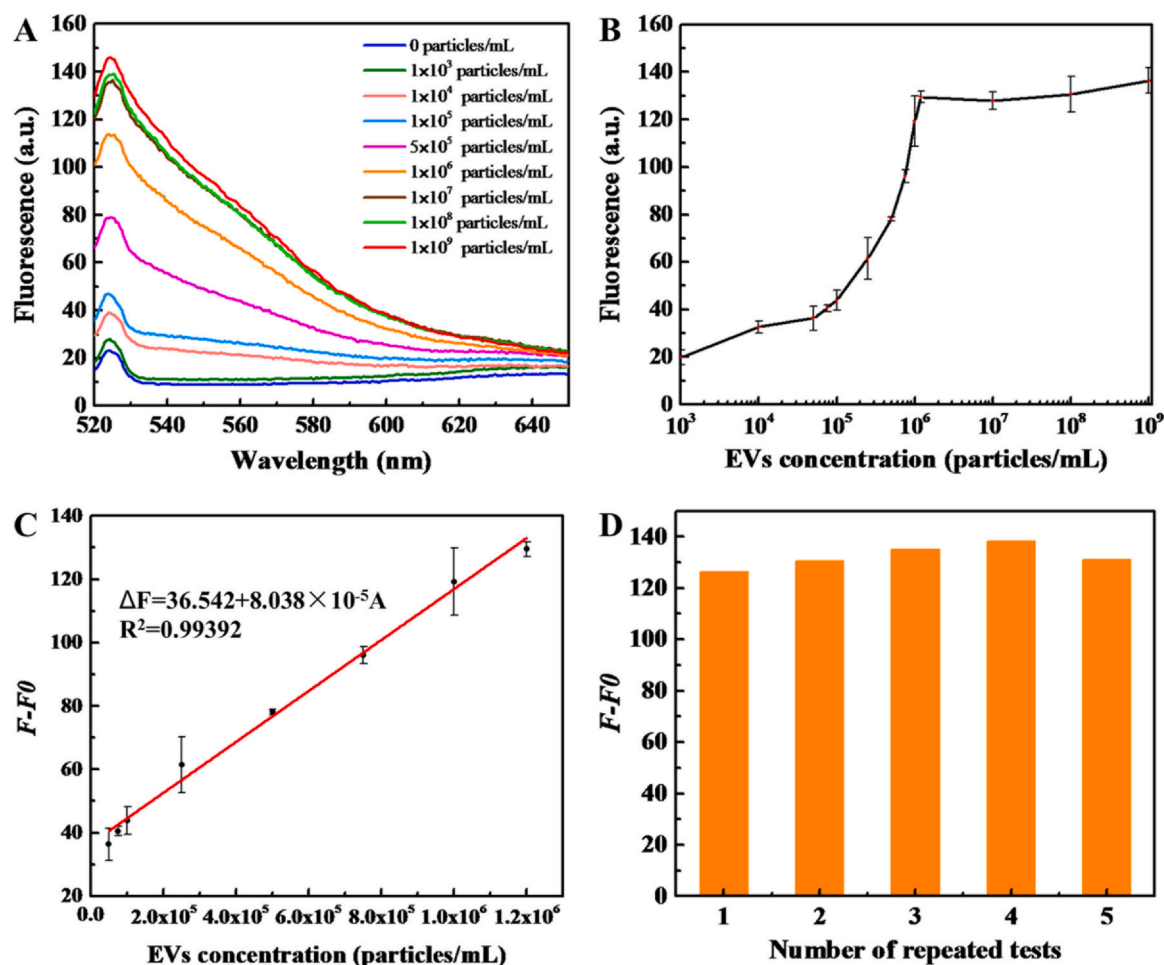


Fig. 7. The relationship between the fluorescent intensity and the concentration of target A549-EVs. (A) Different fluorescent intensity with the concentration of A549-EVs from 0 particles/mL to 1×10^9 particles/mL; (B) Different fluorescent intensity with the concentration of A549-EVs from 1×10^3 particles/mL to 1×10^9 particles/mL; (C) Linear fitting between fluorescence intensity and the concentration of A549-EVs. The error bars were the standard deviation of three repetitive experiments. (D) The reproducibility of the method.

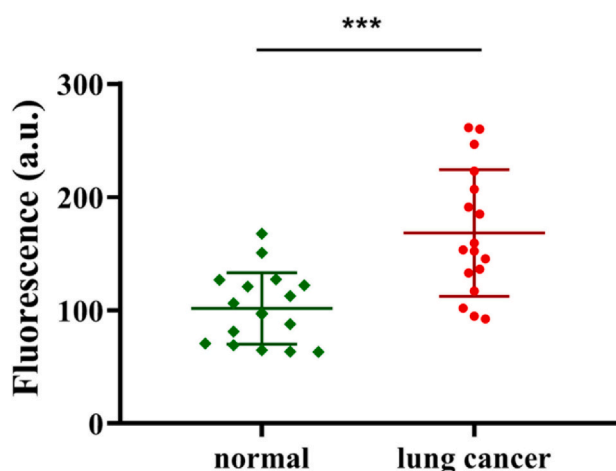


Fig. 8. Fluorescence intensities of clinical serum samples from healthy donors ($n = 17$) compared to that of lung cancer patients ($n = 17$) (***, $P < 0.001$).

Clinical sample analysis

Recent research demonstrated that the analysis of EVs in blood might provide a new diagnostic approach for lung cancer. To evaluate the feasibility of the designed method in the clinical diagnosis, EVs in human plasma samples contained in healthy individuals and lung cancer patients were further analyzed. Before detecting, the original plasma samples were used in this experiment. As shown in Fig. 8, the value of ΔF obtained from the healthy individuals was statistically significantly higher than that obtained from lung cancer patients. The significance of signal suppression between two groups was analyzed using the Mann-Whitney U test ($P < 0.001$). These results indicated that the proposed method could directly distinguish the lung cancer patients and healthy individuals with excellent accuracy, having a great potential for further application in early clinical diagnosis of lung cancers.

Although, there were significant differences between lung cancer patients and healthy individuals, some of lung cancer patients cannot be distinguished. This phenomenon is a common problem faced by clinical examination at present. The main reason is that there are

Table 2
Comparison of different detection schemes of EVs.

Detection methods	Target	Principle	Detection range	Detection limit	Reference
This method	A549-Extracellular vesicles (EVs)	Padlock probe exponential rolling circle amplification	5×10^4 – 1.2×10^6 particles/mL	4.222×10^4 particles/mL	[41]
Surface plasmon resonance (SPR)	MCF-7-exosomes/ MCF-10A-exosomes	Dual gold nanoparticle (AuNP)-assisted signal amplification	N/A	5×10^3 exosomes/mL	[42]
Electrochemical approaches	MCF-7-exosomes	Signal was amplified based on click chemistry and the DNA hybridization chain reaction (HCR)	1.12×10^2 – 1.12×10^8 particles/ μ L	96 particles/ μ L	[43]
	Glioblastoma (GBM)-exosomes	GBMs-exosomes was captured by a peptide through combining with EGFR and EGFRvIII proteins, and Zr-MOFs loaded with methylene blue was combined on the surface of GBMs-exosomes to amplify electrochemical signal	9.5×10^3 – 1.9×10^7 particles/ μ L	7.83×10^3 particles/ μ L	[44]
Fluorescence method	Prostate-specific membrane antigen (PSMA)	Profiling proteins on tumor-derived exosomes was used to detect by tuning the supramolecular interactions of aggregation-induced emission luminogens (AIEgens) and GO with aptamers.	4.07×10^5 – 1.83×10^7 particles/ μ L	3.43×10^5 particles/ μ L	[45]
UV absorbance method	SW480 cell-derived exosomes	Anti-A33 was selected as a probe to capture colorectal cancer (CRC) exosomes and EpCAM aptamer-Au-primer complex was used as a signal probe. The primer could introduce amount of avidin-modified horseradish peroxidase (Av-HRP) which amplified the signal.	9.75×10^3 – 1.95×10^6 particles/ μ L	6.7×10^3 particles/ μ L	[10]
Microfluidic and fluorescence	Lung cancer-exosomes	Polymethyl methacrylate (PMMA) and a nanoporous gold (Au) nanocluster membrane modified with antibody was used to capture exosomes. And AuR-anti-CD81 was used to produce signal.	1×10^3 – 1×10^7 particles/mL	1000 particles/mL	[46]
Surface enhanced Raman scattering (SERS)	MCF-7-cells MCF-7-exosomes	Gold nanoparticles in triangular pyramidal DNA (TP-Au NPs) was used as a Capture probe and a Raman probe which could enhance detecting signals. EpCAM aptamer and Chol-linker DNA was used probe to capture MCF-7-cells or MCF-7-exosomes.	Cells: 3–500 cells/mL Exosomes: 1.0×10^3 – 1.0×10^8 particles/ μ L	Cells: N/A Exosomes: 1.1×10^2 particles/ μ L	[47]
Flow Cytometry approach	Extracellular vesicles (EVs)	A conformation-switchable DNA probe was used to bind EVs and triggered the hybridization chain reaction (HCR) producing signal.	20 μ g/mL–500 μ g/mL	N/A	[48]
Electrical method	Prostate cancer (PCa)-exosomes	Based on a graphene oxide (RGO) field effect transistor (FET) biosensor modified with specific antibody CD63.	33 particles/ μ L– 3.3×10^6 particles/ μ L	33 particles/ μ L	[48]

heterogeneity in lung cancer [40]. One tumor marker cannot be used to distinguish the discrepancy accurately. Therefore, liquid biopsy should be combined with existing diagnostic techniques to further improve the accuracy and sensitivity of cancer detection.

Conclusion

In this work, we established a novel fluorescence method to detect EVs quantitatively. The designed method combined the advantage of aptamer recognition and that of P-ERCA nucleic acid signal amplification strategy. Compared to other reported EVs detecting methods, our method had the following distinctive advantages: (1) The experimental operation was greatly simplified. The whole detecting process only needs two steps: EVs were combined with the aptamer-primer; the reaction of P-ERCA was triggered by the aptamer-primer. The step of preparing circle template could be eliminated before P-ERCA. (2) P-ERCA strategy made the method with extremely high signal amplification efficiency. Under optimum conditions, the proposed method had a good linear relationship for A549-EVs detection in the range from 5×10^4 particles/mL to 1.2×10^6 particles/mL with a detection limit as low as 4.222×10^4 particles/mL. The reproducibility of this method had been verified and the RSD was 3.46% for A549-EVs by evaluating five reduplicate detections. Meanwhile, the sensitivity, dynamic range, and principle of this method were compared with currently reported assays (Table 2), the detection limit and detection range of this method was almost equivalent or had more advantages to some methods. (3) The pretreatment of EVs-aptamer-primer may improve the specificity of the detection and guarantee the stability and repeatability. (4) Moreover, the fluorescence method could distinguish the lung cancer patients from healthy individuals. The positive results were 2.1 times higher than the negative results. Original solution could be detected directly by this method for judging lung cancer. In brief, the method could provide an extraordinary option for the non-invasive liquid biopsy and be promising prospect for the early diagnosis of lung cancer.

Multiple tumor markers and multiple detections will be used to improve detecting efficiency and detecting sensitivity. Artificial intelligence technology also can be used to diagnose lung cancer combining with liquid biopsy.

CRediT authorship contribution statement

Under supervision by Zhiyang Li, Pengfeng Xiao, and Nongyue He, Lei He completed the main experiments and data analysis, Xiaocheng Yu performed sample preparation, Rongrong Huang, Lian Jin, Yuan Liu, Yan Deng, Song Li, Hui Chen, and Zhu Chen give some advice for this paper. All authors read and contributed to the manuscript.

Declaration of Competing Interest

The authors declare that they have no known competing financial interests or personal relationships that could have appeared to influence the work reported in this paper.

Acknowledgements

This study was supported by National Key Research and Development Program of China (No. 2017YFA0205301), the National Natural Scientific Foundation of China (No. 61971216, 81902153 and 62071119), the Jiangsu Province Medical Talent (No. ZDRCA2016065), the Key Research and Development Project of Jiangsu Province (No. BE2019603, BE2020768).

References

- [1] F. Bray, J. Ferlay, I. Soerjomataram, R.L. Siegel, L.A. Torre, A. Jemal, Global cancer statistics 2018: GLOBOCAN estimates of incidence and mortality worldwide for 36 cancers in 185 countries, *CA Cancer J. Clin.* 68 (2018) 394–424, <https://doi.org/10.3322/caac.21492>
- [2] F. Islami, L.A. Torre, A. Jemal, Global trends of lung cancer mortality and smoking prevalence, *Transl. Lung Cancer R.* 4 (2015) 327–338, <https://doi.org/10.3978/j.issn.2218-6751.2015.08.04>
- [3] A. Jemal, R. Siegel, E. Ward, Y. Hao, J. Xu, M.J. Thun, *Cancer Statistics*, 2009, *CA Cancer J. Clin.* 59 (2009) 225–249, <https://doi.org/10.3322/caac.20006>
- [4] D.E. Wood, E.A. Kazerooni, S.L. Baum, G.A. Eapen, D.S. Ettinger, L. Hou, D.M. Jackman, D. Klippenstein, R. Kumar, R.P. Lackner, L.E. Leard, I.T. Lennes, A.N.C. Leung, S.S. Makani, P.P. Massion, P. Mazzone, R.E. Merritt, B.F. Meyers, D.E. Midthun, S. Pipavath, C. Pratt, C. Reddy, M.E. Reid, A.J. Rotter, P.B. Sachs, M.B. Schabath, M.L. Schiebler, B.C. Tong, W.D. Travis, B. Wei, S.C. Yang, K.M. Gregory, M. Hughes, Lung cancer screening, version 3.2018, NCCN clinical practice guidelines in oncology, *J. Natl. Compr. Cancer Netw.* 16 (2018) 412–441, <https://doi.org/10.6004/jnccn.2018.0020>
- [5] L. Chen, H. Jing, Y. Gong, A.L. Tam, J. Stewart, G. Staerckel, M. Guo, Diagnostic efficacy and molecular testing by combined fine-needle aspiration and core needle biopsy in patients with a lung nodule, *Cancer Cytopathol.* 128 (2020) 201–206, <https://doi.org/10.1002/cncy.22234>
- [6] S. Pan, Y. Zhang, M. Huang, Z. Deng, A. Zhang, L. Pei, L. Wang, W. Zhao, L. Ma, Q. Zhang, D. Cui, Urinary exosomes-based engineered nanovectors for homologically targeted chemo-chemodynamic prostate cancer therapy via abrogating EGFR/AKT/NF- κ B/I κ B signaling, *Biomaterials* 275 (2021) 120946, <https://doi.org/10.1016/j.biomaterials.2021.120946>
- [7] S. Pan, L. Pei, A. Zhang, Y. Zhang, C. Zhang, M. Huang, Z. Huang, Bin Liu, L. Wang, L. Ma, Q. Zhang, D. Cui, Passion fruit-like exosome-PMA/Au-BSA@Ce6 nanovehicles for real-time fluorescence imaging and enhanced targeted photodynamic therapy with deep penetration and superior retention behavior in tumor, *Biomaterials* 230 (2020) 119606, <https://doi.org/10.1016/j.biomaterials.2019.119606>
- [8] H. Wei, X. Qian, F. Xie, D. Cui, Isolation of exosomes from serum of patients with lung cancer: a comparison of the ultra-high speed centrifugation and precipitation methods, *Ann. Transl. Med.* 9 (2021) 882, <https://doi.org/10.21037/atm-21-2075>
- [9] G. van Niel, G. D'Angelo, G. Raposo, Shedding light on the cell biology of extracellular vesicles, *Nat. Rev. Mol. Cell Biol.* 19 (2018) 213–228, <https://doi.org/10.1038/nrm.2017.125>
- [10] Z. Huang, Q. Lin, X. Ye, B. Yang, R. Zhang, H. Chen, W. Weng, J. Kong, Terminal deoxynucleotidyl transferase based signal amplification for enzyme-linked aptamer-sorbent assay of colorectal cancer exosomes, *Talanta* 218 (2020) 121089, <https://doi.org/10.1016/j.talanta.2020.121089>
- [11] P. Zhang, M. He, Y. Zeng, Ultrasensitive microfluidic analysis of circulating exosomes using a nanostructured graphene Oxide/Polydopamine coating, *Lab Chip* 16 (2016) 3033–3042, <https://doi.org/10.1039/c6lc00279j>
- [12] J. Ko, M.A. Hemphill, D. Gabrieli, L. Wu, V. Yelleswarapu, G. Lawrence, W. Pennycook, A. Singh, D.F. Meaney, D. Issadore, Smartphone-enabled optofluidic exosome diagnostic for concussion recovery, *Sci. Rep.* 6 (2016) 31215, <https://doi.org/10.1038/srep31215>
- [13] X. Xu, H. Li, D. Hasan, R.S. Ruoff, A.X. Wang, D.L. Fan, Near-Field enhanced plasmonic-magnetic bifunctional nanotubes for single cell bioanalysis, *Adv. Funct. Mater.* 23 (2013) 4332–4338, <https://doi.org/10.1002/adfm.201203822>
- [14] D.L.M. Rupert, C. Lässer, M. Eldh, S. Block, V.P. Zhdanov, J.O. Lotvall, M. Bally, F. Höök, Determination of exosome concentration in solution using surface plasmon resonance spectroscopy, *Anal. Chem.* 86 (2014) 5929–5936, <https://doi.org/10.1021/ac500931f>
- [15] L. Zhu, K. Wang, J. Cui, H. Liu, X. Bu, H. Ma, W. Wang, H. Gong, C. Lausted, L. Hood, G. Yang, Z. Hu, Label-free quantitative detection of tumor-derived exosomes through surface plasmon resonance imaging, *Anal. Chem.* 86 (2014) 8857–8864, <https://doi.org/10.1021/ac5023056>
- [16] H. Dong, H. Chen, J. Jiang, H. Zhang, C. Cai, Q. Shen, Highly sensitive electrochemical detection of tumor exosomes based on aptamer recognition-induced multi-DNA release and cyclic enzymatic amplification, *Anal. Chem.* 90 (2018) 4507–4513, <https://doi.org/10.1021/acs.analchem.7b04863>
- [17] T. Kilic, A.T.D.S. Valinhas, I. Wall, P. Renaud, S. Carrara, Label-free detection of hypoxia-induced extracellular vesicle secretion from MCF-7 cells, *Sci. Rep.* 8 (2018) 9402, <https://doi.org/10.1038/s41598-018-27203-9>
- [18] S. Jeong, J. Park, D. Pathania, C.M. Castro, R. Weissleder, H. Lee, Integrated magneto-electrochemical sensor for exosome analysis, *ACS Nano* 10 (2016) 1802–1809, <https://doi.org/10.1021/acsnano.5b07584>
- [19] K. Boriachek, M.N. Islam, V. Gopalan, A.K. Lam, N.T. Nguyen, M.J.A. Shiddiky, Quantum dot-based sensitive detection of disease specific exosome in serum, *Analyst* 142 (2017) 2211–2219, <https://doi.org/10.1039/C7AN00672A>
- [20] S. Wang, L. Zhang, S. Wan, S. Cansiz, C. Cui, Y. Liu, R. Cai, C. Hong, I.T. Teng, M. Shi, Y. Wu, Y. Dong, W. Tan, Aptasensor with expanded nucleotide using DNA nanotetrahedra for electrochemical detection of cancerous exosomes, *ACS Nano* 11 (2017) 3943–3949, <https://doi.org/10.1021/acsnano.7b00373>
- [21] Y.G. Zhou, R.M. Mohamadi, M. Poudineh, L. Kermanshah, S. Ahmed, T.S. Safaei, J. Stojic, R.K. Nam, E.H. Sargent, S.O. Kelley, Interrogating circulating microRNAs and exosomes using metal nanoparticles, *Small* 12 (2015) 727–732, <https://doi.org/10.1002/smll.201502365>

- [22] Q. Zhou, A. Rahimian, K. Son, D.S. Shin, T. Patel, A. Revzin, Development of an aptasensor for electrochemical detection of exosomes, *Methods* 97 (2016) 88–93, <https://doi.org/10.1016/j.jymeth.2015.10.012>
- [23] P. Liu, X. Qian, X. Li, L. Fan, X. Li, D. Cui, Y. Yan, Enzyme-free electrochemical biosensor based on localized DNA cascade displacement reaction and versatile DNA nanosheets for ultrasensitive detection of exosomal microRNA, *ACS Appl. Mater. Interfaces* 12 (2020) 45648–45656, <https://doi.org/10.1021/acsami.0c14621>
- [24] R. Huang, L. He, Y. Xia, H. Xu, C. Liu, H. Xie, S. Wang, L. Peng, Y. Liu, Y. Liu, N. He, Z. Li, A sensitive aptasensor based on a hemin/G-quadruplex-assisted signal amplification strategy for electrochemical detection of gastric cancer exosomes, *Small* 15 (2019) 1900735, <https://doi.org/10.1002/smll.201900735>
- [25] X. Chen, J. Lan, Y. Liu, L. Li, L. Yan, Y. Xia, F. Wu, C. Li, S. Li, J. Chen, A paper-supported aptasensor based on upconversion luminescence resonance energy transfer for the accessible determination of exosomes, *Biosens. Bioelectron.* 102 (2018) 582–588, <https://doi.org/10.1016/j.bios.2017.12.012>
- [26] N. He, Lei He, Z. Li, Aptamers against A549-extracellular vesicles using for detecting of lung cancer and its application, patent, CN 202110689330.6.
- [27] Z. Li, C. Hu, J. Jia, Y. Xia, H. Xie, M. Shen, R. Huang, L. He, C. Liu, S. Wang, B. Chen, N. He, Establishment and evaluation of a simple size-selective method for exosome enrichment and purification, *J. Biomed. Nanotechnol.* 15 (2019) 1090–1096, <https://doi.org/10.1166/jbnn.2019.2768>
- [28] Y. Wan, G. Cheng, X. Liu, S. Hao, M. Nisic, C. Zhu, Y. Xia, W. Li, Z. Wang, W. Zhang, S.J. Rice, A. Sebastian, I. Albert, C.P. Belani, S. Zheng, Rapid magnetic isolation of extracellular vesicles via lipid-based nanoprobe, *Nat. Biomed. Eng.* 1 (2017) 0058, <https://doi.org/10.1038/s41551-017-0058>
- [29] G. Huang, G. Lin, Y. Zhu, W. Duan, D. Jin, Emerging technologies for profiling extracellular vesicle heterogeneity, *Lab Chip* 20 (2020) 2423–2437, <https://doi.org/10.1039/d0lc00431f>
- [30] Y. Pang, J. Shi, X. Yang, C. Wang, Z. Sun, R. Xiao, Personalized detection of circling exosomal PD-L1 based on Fe₃O₄@TiO₂ isolation and SERS immunoassay, *Biosens. Bioelectron.* 148 (2020) 111800, <https://doi.org/10.1016/j.bios.2019.111800>
- [31] Z. Fan, J. Yu, J. Lin, Y. Liu, Y. Liao, Exosome-specific tumor diagnosis via biomedical analysis of exosome-containing microRNA biomarker, *Analyst* 119 (2019) 5856–5865, <https://doi.org/10.1039/C9AN00777F>
- [32] B. Liu, G. Qiao, W. Cao, C. Li, S. Pan, L. Wang, Y. Liu, L. Ma, D. Cui, Proteomics analyses reveal functional differences between exosomes of mesenchymal stem cells derived from the umbilical cord and those derived from the adipose tissue, *Cell J.* 23 (2021) 75–84, <https://doi.org/10.22074/cellj.2021.6969>
- [33] H. Liu, L. Li, L. Duan, X. Wang, Y. Xie, L. Tong, Q. Wang, B. Tang, High specific and ultrasensitive isothermal detection of microRNA by padlock probe-based exponential rolling circle amplification, *Anal. Chem.* 85 (2013) 7941–7947, <https://doi.org/10.1021/ac401715k>
- [34] M. Liss, B. Petersen, H. Wolf, E. Prohaska, An aptamer-based quartz crystal protein biosensor, *Anal. Chem.* 74 (2002) 4488–4495, <https://doi.org/10.1021/ac011294p>
- [35] J. Zhou, J. Rossi, Aptamers as targeted therapeutics: current potential and challenges, *Nat. Rev. Drug Discov.* 16 (2017) 181–202, <https://doi.org/10.1038/nrd.2016.199>
- [36] Y. Zhang, B.S. Lai, M. Juhas, Recent advances in aptamer discovery and applications, *Molecules* 24 (2019) 941, <https://doi.org/10.3390/molecules24050941>
- [37] D. Li, T. Zhang, F. Yang, R. Yuan, Y. Xiang, Efficient and exponential rolling circle amplification molecular network leads to ultrasensitive and label-free detection of MicroRNA, *Anal. Chem.* 92 (2020) 2074–2079, <https://doi.org/10.1021/acs.analchem.9b04585>
- [38] X.Y. Li, Y.X. Cui, Y.C. Du, A.N. Tang, D.M. Kong, Label-free telomerase detection in single cell using a five-base telomerase product-triggered exponential rolling circle amplification strategy, *ACS Sens.* 4 (2019) 1090–1096, <https://doi.org/10.1021/acssensors.9b00334>
- [39] X. Li, X. Ni, F. Cui, Q. Qiu, X. Chen, H. Huang, A logic dual-channel detection of Hox transcript antisense intergenic RNA using graphene switch and padlock probe-based exponential rolling circle amplification assay, *Sens. Actuators B Chem.* 340 (2021) 129931, <https://doi.org/10.1016/j.snb.2021.129931>
- [40] M. Xu, D.C. Wang, X. Wang, Y. Zhang, Correlation between mucin biology and tumor heterogeneity in lung cancer, *Semin. Cell Dev. Biol.* 64 (2017) 73–78, <https://doi.org/10.1016/j.semcdb.2016.08.027>
- [41] Q. Wang, L. Zou, X. Yang, X. Liu, W. Nie, Y. Zheng, Q. Cheng, K. Wang, Direct quantification of cancerous exosomes via surface plasmon resonance with dual gold nanoparticle-assisted signal amplification, *Biosens. Bioelectron.* 135 (2019) 129–136, <https://doi.org/10.1016/j.bios.2019.04.013>
- [42] Y. An, T. Jin, Y. Zhu, F. Zhang, P. He, An ultrasensitive electrochemical aptasensor for the determination of tumor exosomes based on click chemistry, *Biosens. Bioelectron.* 142 (2019) 111503, <https://doi.org/10.1016/j.bios.2019.111503>
- [43] Z. Sun, L. Wang, S. Wu, Y. Pan, Y. Dong, S. Zhu, J. Yang, Y. Yin, G. Li, An electrochemical biosensor designed by using Zr-based metal-organic frameworks for the detection of glioblastoma-derived exosomes with practical application, *Anal. Chem.* 92 (2020) 3819–3826, <https://doi.org/10.1021/acs.analchem.9b05241>
- [44] B. Li, C. Liu, W. Pan, J. Shen, J. Guo, T. Luo, J. Feng, B. Situ, T. An, Y. Zhang, L. Zheng, Facile fluorescent aptasensor using aggregation-induced emission luminogens for exosomal proteins profiling towards liquid biopsy, *Biosens. Bioelectron.* 168 (2020) 112520, <https://doi.org/10.1016/j.bios.2020.112520>
- [45] Q. Yang, L. Cheng, L. Hu, D. Lou, T. Zhang, J. Li, Q. Zhu, F. Liu, An integrative microfluidic device for isolation and ultrasensitive detection of lung cancer-specific exosomes from patient urine, *Biosens. Bioelectron.* 163 (2020) 112290, <https://doi.org/10.1016/j.bios.2020.112290>
- [46] X. Zhang, C. Liu, Y. Pei, W. Song, S. Zhang, Preparation of a novel raman probe and its application in the detection of circulating tumor cells and exosomes, *ACS Appl. Mater. Interfaces* 11 (2019) 28671–28680, <https://doi.org/10.1021/acsami.9b09465>
- [47] W. Shen, K. Guo, G.B. Adkins, Q. Jiang, Y. Liu, S. Sedano, Y. Duan, W. Yan, S.E. Wang, K. Bergersen, D. Worth, E.H. Wilson, W. Zhong, A single extracellular vesicle (EV) flow cytometry approach to reveal EV heterogeneity, *Angew. Chem. Int. Ed.* 57 (2018) 15675–15680, <https://doi.org/10.1002/anie.201806901>
- [48] Y. Yu, Y.T. Li, D. Jin, F. Yang, D. Wu, M.M. Xiao, H. Zhang, Z.Y. Zhang, G.J. Zhang, Electrical and label-free quantification of exosomes with a reduced graphene oxide field effect transistor biosensor, *Anal. Chem.* 91 (2019) 10679–10686, <https://doi.org/10.1021/acs.analchem.9b01950>